HHS Public Access

Author manuscript

J Biomed Mater Res A. Author manuscript; available in PMC 2021 October 01.

Published in final edited form as:

J Biomed Mater Res A. 2021 October ; 109(10): 1828–1839. doi:10.1002/jbm.a.37175.

Suppression of NF-κB-induced chronic inflammation mitigates inflammatory osteolysis in the murine continuous polyethylene particle infusion model

Takeshi Utsunomiya[1], **Ning Zhang**[1], **Tzuhua Lin**[1], **Yusuke Kohno**[1], **Masaya Ueno**[1], **Masahiro Maruyama**[1], **Ejun Huang**[1], **Claire Rhee**[1], **Zhenyu Yao**[1], **Stuart B. Goodman**[1,2]

[1]Department of Orthopaedic Surgery, Stanford University, Stanford, California

[2]Bioengineering, Stanford University, Stanford, California

Abstract

Wear particle-associated bone loss (periprosthetic osteolysis) constrains the longevity of total joint arthroplasty (TJA). Wear particles induce a prolonged upregulation of nuclear factor kappa B (NF-κB) signaling in macrophages and osteoclasts. Synthetic double-stranded oligodeoxynucleotides (ODNs) can prevent the binding of NF-κB to the promoter regions of targeted genes and inhibit genetic activation. We tested the hypothesis that polyethylene-particle induced chronic inflammatory bone loss could be suppressed by local delivery of NF-κB decoy ODNs in murine in vivo model. Polyethylene particles were continuously infused into the medullary cavity of the distal femur for 6 weeks to induce chronic inflammation, and micro-computational tomography and immunohistochemical analysis were performed. Particle-induced chronic inflammation resulted in lower BMD values, an increase in osteoclastogenesis and nuclear translocation of p65, a prolonged M1 pro-inflammatory macrophage phenotype, and a decrease of M2 anti-inflammatory macrophage phenotype. Delayed timing of local infusion of NF-κB decoy ODN for the last 3 weeks reversed polyethylene-particle associated chronic inflammatory bone loss and facilitated bone healing. This study demonstrated that polyethylene-particle associated chronic inflammatory osteolysis can be effectively modulated via interference with the NF-κB pathway; this minimally invasive intervention could potentially be an efficacious therapeutic strategy for periprosthetic osteolysis after TJA.

Keywords

bone healing; inflammation; macrophage; oligodeoxynucleotide; osteolysis

1 | INTRODUCTION

Total joint arthroplasty (TJA) is a common surgical option that generally provides highly successful outcomes in patients with advanced degenerative arthritis. Although TJA has

Correspondence: Prof. Stuart B. Goodman, Department of Orthopaedic Surgery, Stanford University School of Medicine, 300 Pasteur Drive, Edwards Building, Stanford University, Stanford, CA 94305,USA. goodbone@stanford.edu.

DATA AVAILABILITY STATEMENT

No data are available because we cannot share the dataset according to rules of our institution.

demonstrated long-term success, wear particles and other byproducts from TJA can induce chronic inflammation and bone resorption.[1] Since revision TJA for osteolysis is technically more demanding with higher complication rates compared to primary TJA,[2] new strategies for reducing osteolysis due to wear particles and other byproducts are required to improve the survivorship after TJA.

Wear particles induce a biological reaction characterized by prolonged upregulation of nuclear factor kappa B (NF-κB) that is, the essential factor for transcriptional activity for pro-inflammatory cytokines, chemokines and other pro-inflammatory molecules.[3–5] Wear particles also activate macrophages that stimulate both paracrine and autocrine cell interactions and initiate the inflammatory cascade.[6] This instigates the differentiation, maturation and activation of osteoclasts, resulting in peri-prosthetic bone resorption.[7,8] In addition, macrophages play an important role in helping to recruit and differentiate mesenchymal stem cells (MSCs) to stimulate bone healing.[9] Therefore, immunomodulation to sense and regulate increased NF-κB signaling could be a strategy to mitigate particle-associated chronic inflammatory bone loss.

NF-κB decoy oligodeoxynucleotides (ODNs) can prevent the binding of essential transcriptional factors, such as NF-κB p65:IκB complex to the promoter regions of targeted genes in the nucleus, leading to the suppression of genetic activation.[10,11] Using NF-κB decoy ODNs, acute polyethylene wear particle-induced osteolysis was reduced in both a murine calvarial model[12] and a murine femoral intramedullary continuous polyethylene particle infusion model (Table 1).[13,14] Using a calvarial model, ultra-high molecular weight polyethylene (UHMWPE) particles were injected onto a flat bone subcutaneously on day 1, and NF-κB decoy ODN was also locally injected daily from day 1 to day 14.[12] Using the murine continuous femoral particle infusion model, Lin et al also reported two studies in which both UHMWPE particles and NF-κB decoy ODN were continuously infused into the medullary cavity of the distal femur from day 1 to day 21,[13] and day 1-day 28,[14] respectively. These previous studies simulated an acute and relatively short-term inflammatory response to polyethylene particles, which is more clinically meaningful to the initial osseointegration of implants. Whether these same principles are applicable to chronic inflammation, which could result in continued bone loss, implant loosening and clinical failure, is unknown. Considering that larger amounts of wear particles and other byproducts are created after the periods of initial implantation of prosthetic surgery, the longer experimental period and the delayed timing of therapeutic intervention are desirable to address the effects of local delivery of NF-κB decoy ODNs on chronic inflammatory bone loss. We hypothesized that osteolysis due to chronic inflammation caused by the continuous infusion of polyethylene particles for 6 weeks could be suppressed by local infusion of NF-κB Decoy ODNs during the last 3 weeks using the murine continuous polyethylene particle infusion model.

The purpose of our study is to test this hypothesis using our established in vivo model.

2 | MATERIALS AND METHODS

2.1 | NF-κB decoy ODN

The sequences of the NF-κB decoy ODN in the current study are 5′-CCTTGAAGGGATTTCCCTCC-3′ and 3′-GGAACTTCCCTTCCCTAAAGGGAGG-5′.[15] The NF-κB decoy ODNs were produced by Integrated DNA technologies (IDT, Coralville, IA) in HPLC grade.

2.2 | UHMWPE particles

We prepared the polyethylene particles as previously described.[16,17] Briefly, we washed and resuspended Ceridust 3,610 polyethylene particles (Clariant Corporation, CA) using 100% ethanol. These polyethylene particles were then filtrated through a filter with the pores of 20 μm to remove the larger size of particles. Finally, the size of filtered polyethylene particles was measured as 4.62 ± 3.76 μm using a scanning electron microscope (Zeiss Sigma FESEM, Zeiss Sigma, CA) in the Cell Science Image Facility at Stanford University.

The filtered particles were vacuum-dried and resuspended for 3 days in phosphate-buffered saline (PBS) containing 5% bovine serum albumin (BSA, Thermo Fisher Scientific) at a concentration of approximately 3.1×10^{10} particles/ml. We confirmed the sterility of the polyethylene particles using PYROGENT™-5000 Bulk Kinetic Turbidimetric LAL assay for endotoxin testing (Lonza, Portsmouth, NH). [16,17] To generate contaminated polyethylene particles, 10 ng/ml of lipopolysaccharides (LPS, Sigma–Aldrich, St Louis, MO) were then added. [18] Contaminated polyethylene particles were filled into Alzet mini-osmotic pumps (Model 2006, DURECT corporation, Cupertino, CA). The contaminated polyethylene particles were infused at a constant pumping rate (mean, 0.15 μl/hr) for total 6 weeks. Therefore, the total amount of contaminated particles that was infused per mouse for 6 weeks was 4.7×10^9 particles theoretically.

2.3 | Murine model of polyethylene particle-associated osteolysis and experimental design

The experimental design of this study was approved by the Institutional Administration Panel for Laboratory Animal Care at Stanford University (Protocol number: 17566) and Institutional Guidelines for the Care and Use of Laboratory Animals were observed in all aspects of this project (Male BALB/c mice with 11-12 weeks old, Jackson Laboratory, Bar Harbor, ME). We conducted all the primary surgeries within 2 weeks after arrival to our institution. The mice were kept on a 12-hr light-and-dark cycle and they were able to access a standard diet with food and water ad libitum.

We conducted surgeries to accomplish the murine in vivo model in which polyethylene particles were continuously infused into the medullary cavity of the distal femur as previously described (Figure 1).[13,14,19–25] Briefly, under inhalation anesthesia with isoflurane in 100% oxygen at a flow of 1 L/min on a warm surgical station for small animals, we approached the right knee joint via a lateral parapatellar incision. A series of needles (25, 23, and 22 gauges) was sequentially used to penetrate the intercondylar notch into the medullary space. A hollow titanium rod (length: 6 mm, diameter:23 gauge) was then

press-fit into the cavity of the distal femur. We implanted an osmotic pump that contained polyethylene particles in PBS into the dorsal side of mouse subcutaneously through another skin incision around the right shoulder. Using a vinyl catheter tubing, we connected a pump with a hollow titanium rod that was press-fit into the medullary cavity. We closed skin incisions with 5–0 Ethilon sutures and we used subcutaneous buprenorphineSR injections (0.1 mg/kg) for analgesia after the surgeries. Each mouse was able to access the food and water freely in their own cage.

At primary surgery, we implanted the pumps with 10% BSA/PBS with/without contaminated polyethylene particles (cPE, 1.25% of polyethylene particles and 10 ng/ml of LPS). For the delivery of the NF-κB decoy ODN at 3 weeks after primary surgery, pumps were replaced with new ones filled with both 10% BSA/PBS and NF-κB Decoy ODN (50 μM)[13,14] with/without cPE, which were infused together for three more weeks (Figure 1).

Thus, there were four groups with/without cPE and with/without treatment of NF-κB Decoy ODN as follows: (a) Treatment group without cPE, (b) infusion of decoy ODN at 3 weeks after primary surgery without cPE, (c) treatment group with cPE, and (d) infusion of decoy ODN at 3 weeks after primary surgery with cPE (Figure 1). Power analysis was carried out to determine a sufficient number of mice for this in vivo study, based on detecting a significant difference of 1.3 *SD* (effect size of 1.3) with a power of 90% (alpha = 0.05, beta = 0.10). Changes in bone morphometric parameters were based on results of histomorphometry and micro-computational tomography (MicroCT) from our previous studies. The power analysis concluded that an $n = 7$ animals were necessary for these in vivo animals. Thus, each group included seven mice.

2.4 | Micro-computational tomography

Mice were euthanized with exposure to CO_2 followed by cervical dislocation, and all the implants including the hollow titanium rod, a vinyl catheter tubing and a pump were detached before MicroCT scanning 6 weeks after the primary surgery. MicroCT scans were performed using the eXplore Locus RS150 microCT (GE Healthcare, Fairfield, CT) with 49 μm resolution. A three-dimension (3D) region of interest (ROI, height: 3 mm, width: 4 mm, depth: 3 mm) was generated within the diaphysis. The distal end of 3D-ROI was set 3 mm proximally from the distal end of the femoral condyles along the longitudinal axis of the femur (Figure 2a).[14,22] We quantified the bone mineral density (BMD, mg/ mm^3) using the GEMS MicroView software in which threshold was set as 700 HU.

2.5 | Tissue processing and histological analysis

We excised the operated femurs at 6 weeks after the primary surgery, after performing the microCT scans. We fixed the femurs in 4% paraformaldehyde overnight followed by decalcification of the femurs using 0.5 M ethylenediamine tetra acetic acid (EDTA) for 2 weeks. We then placed the femurs in embedding medium (optimal cutting temperature or OCT) (Tissue Plus®, Fisher HealthCare, Hampton, NH) for frozen specimens. Finally, we prepared transverse sections with 10 μm-thickness using the region of interest located 3 mm proximally from the distal end of femoral condyles for following immunohistochemistry.[14]

2.6 | Immunohistochemistry and measurement

Osteoclast-like cells and osteoblast-like cells were determined as previously described.[12,14,22] Briefly, leukocyte tartrate resistant acid phosphatase (TRAP) staining kit (Sigma-Aldrich, St. Louis, MO) was used to identify osteoclast-like cells with multinuclei stained with brown, which were located on the bone perimeter within the resorption lacunae. Using three randomly selected views with ×200 magnification in each specimen, in a blind manner, two investigators manually counted the number of TRAP staining positive cells, which were finally normalized by the bone area measured using the ImageJ software (National Institutes of Health). In different sections, we also identified osteoblast-like cells using anti-alkaline phosphatase (ALP) antibody (1-Step™ NBT/BCIP Substrate Solution, Thermo Scientific, Rockford, IL).[26] Using the entire image of each specimen with ×100 magnification, the percentage of brown, positively stained area for ALP was quantified based on the entire area of each section measured using the ImageJ software (National Institute of Health).[26] Color threshold of ALP staining positive area was determined by consensus of three of the investigators.

For the preparation for detection of macrophages, we exposed the sections to 5% BSA as blocking buffer for 30 min at room temperature. We then incubated the sections with each of the primary and secondary antibodies for 1 hr, respectively. We identified macrophages by the immunofluorescence staining with rat anti-mouse F4/80 monoclonal antibody (CI: A3-1, Bio-Rad) followed by Alexa Fluor ® 594 conjugated goat anti-rat IgG (Invitrogen, CA). To identify the M1-pro-inflammatory macrophage phenotype, we also stained the sections with rabbit anti-mouse inducible nitric oxide synthase (iNOS) polyclonal antibody (Abcam, Cambridge, United Kingdom) followed by Alexa Fluor ® 488 conjugated goat anti-rabbit IgG (Invitrogen, CA).[26] We mounted the slides with Pro-Long Gold Antifade Mount with DAPI (Life Technologies, Grand Island, NY) and we observed the photomicrographs under a fluorescence microscope (Digital Microscope, Keyence, IL). The number of cells positively stained with F4/80 and the number of cells double positively stained with both F4/80 and iNOS (the M1 pro-inflammatory macrophage phenotype) were manually counted in three randomly selected views of each specimen with ×200 magnification by ImageJ software (National Institute of Health). Finally, we quantified the proportion of M1 pro-inflammatory macrophages based on the following calculation: The number of cells double positively stained with both F4/80 and iNOS divided by the sum of the number of cells stained with F4/80 and the number of cells double positively stained with both F4/80 and iNOS.

Different sections were also exposed to 5% BSA as blocking buffer for 30 min at room temperature followed by incubation with each of the primary and secondary antibodies for 1 hr, respectively. We identified macrophages by the immunofluorescence staining with rat anti-mouse F4/80 monoclonal antibody (CI: A3-1, Bio-Rad) followed by Alexa Fluor ® 594 conjugated goat anti-rat IgG (Invitrogen, CA). We stained these sections with rabbit anti-mouse liver Arginase (Arg1) polyclonal antibody (Abcam, Cambridge, United Kingdom) followed by Alexa Fluor ® 488 conjugated goat anti-rabbit IgG (Invitrogen, CA) as a marker for the M2 anti-inflammatory macrophage phenotype.[26] We mounted the slides with ProLong Gold Antifade Mount with DAPI (Life Technologies, Grand Island, NY) and

we observed the photomicrographs under a fluorescence microscope (Digital Microscope, Keyence, IL). The number of cells positively stained with F4/80 and the number of cells double positively stained with both F4/80 and Arg1 (the M2 anti-inflammatory macrophage phenotype) were manually counted in three randomly selected views of each specimen with ×200 magnification by ImageJ software (National Institute of Health). Finally, we quantified the proportion of M2 anti-inflammatory macrophages based on the following calculation: The number cells double positively stained with both F4/80 and Arg1 divided by the sum of the number of cells positively stained with F4/80 and the number of cells double positively stained with both F4/80 and Arg1.

For monitoring nuclear translocation of p65 (the core component of NF-κB),[27] we exposed other sections to 5% BSA as blocking buffer for 30 min at room temperature followed by incubation with each of the primary and secondary antibodies for 1 hr, respectively. We stained these sections with rabbit Anti-NF-κB p65 (phospho S276) antibody (Abcam, Cambridge, United Kingdom) followed by Goat antirabbit IgG H&L (Alexa Fluor ® 647) preabsorbed (Abcam, Cambridge, United Kingdom). We mounted the slides with ProLong Gold Antifade Mount with DAPI (Life Technologies, Grand Island, NY) and we observed the photomicrographs under a fluorescence microscope with ×200 magnification (Digital Microscope, Keyence, IL) to compare nuclear translocation of p65 in each group.

2.7 | Statistical analysis

One-way analysis of variance with Tukey's post-hoc test was conducted using the GraphPad Prism 7 (San Diego, CA) to quantify the results of MicroCT scanning and immunohistochemistry staining. Data are presented as mean and standard deviations. The difference was considered significant when the p-value was <.05.

3 | RESULTS

None of the mice demonstrated evidence of infection and ambulated relatively normally several days after the surgical procedure.

3.1 | Local delivery of NF-κB decoy ODN reversed bone loss induced by cPE in chronic inflammation

BMD in the treatment group with cPE (533.4 ± 14.2 mg/ mm^3) was significantly reduced compared with that in the treatment group without cPE (560.9 ± 9.3 mg/ mm^3, $p = 0.004$). BMD in the decoy ODN group without cPE (573.1 ± 21.2 mg/ mm^3) was significantly increased compared with that in the treatment group without cPE (533.4 ± 14.2 mg/ mm^3, $p = 0.0152$). BMD in the decoy ODN group with cPE (548.2 ± 14.7 mg/ mm^3) was significantly increased compared with that in the treatment group with cPE (533.4 ± 14.2 mg/ mm^3, $p = 0.0167$). There was no statistically significant difference of BMD between the treatment group without cPE (560.9 ± 9.3 mg/ mm^3) and the decoy ODN group with cPE (548.2 ± 14.7 mg/ mm^3, $p = 0.5284$) (Figure 2b).

3.2 | Local delivery of NF-κB decoy ODN reduced osteoclastogenesis induced by cPE in chronic inflammation

The number of cells positively stained with TRAP in the treatment group with cPE was significantly increased compared with that in the treatment group without cPE ($p = 0.002$). The number of cells positively stained with TRAP in the decoy ODN group with cPE was significantly decreased compared with that in the treatment group with cPE ($p = 0.0068$). There was no statistical difference of the number of cells positively stained with TRAP between the treatment group without cPE and the Decoy ODN group with cPE ($p = 0.8727$) (Figure 3a).

3.3 | Local delivery of NF-κB decoy ODN increased the percentage of ALP staining positive area in chronic inflammation

The percentage of ALP staining positive area based on the whole section of each specimen in the decoy ODN group without cPE was significantly increased compared with that in the treatment group without cPE ($p < 0.0001$). The percentage of ALP staining positive area in the entire section in the decoy ODN group with cPE was significantly increased compared with that in the treatment groups with/without cPE ($p = 0.0003$, $p = 0.0098$, respectively) (Figure 3b).

3.4 | Macrophage phenotype

Total number of macrophages of each section (the sum of the number of cells positively stained with F4/80 and the number of cells double positively stained with both F4/80 and iNOS in Figure 4b, and the sum of the number of cells positively stained with F4/80 and the number of cells double positively stained with both F4/80 and Arg1 in Figure 5b) in the treatment group with cPE was significantly increased compared to those of other groups ($p < 0.0001$). The proportion of M1 pro-inflammatory macrophages (based on the following calculation: the number of cells double positively stained with both F4/80 and iNOS divided by the sum of the number of cells positively stained with F4/80 and the number of cells double positively stained with both F4/80 and iNOS) in the treatment group with cPE was significantly increased compared to that of the treatment group without cPE ($p = 0.0078$), that of the decoy ODN group without cPE ($p = 0.0265$) and that of the decoy ODN group with cPE ($p = 0.0013$) (Figure 4c).

Using different sections, the proportion of M2 anti-inflammatory macrophages (based on the following calculation: The number cells of double positively stained with both F4/80 and Arg1 divided by the sum of the number of cells positively stained with F4/80 and the number of cells double positively stained with both F4/80 and Arg1) in the treatment group with cPE was significantly decreased compared to those of all other groups ($p < 0.0001$) (Figure 5c).

3.5 | Nuclear translocation of p65

The sections were stained with anti-p65 staining and nuclei were visualized with DAPI (Figure 6). In merged images, the overlapping of anti-p65 staining and nuclei stained with DAPI indicated that p65 was located within nuclei (nuclear translocation of p65). In the treatment group with cPE, nuclear translocation of p65 was markedly observed (Figure 6).

On the other hand, in the other groups, anti-p65 staining was located mainly outside of nuclei stained with DAPI. Notably, in NF-κB decoy ODN treatment groups, the overlapping of anti-p65 staining and nuclei stained with DAPI was less compared to that in the treatment with cPE group, suggesting that local infusion of NF-κB decoy ODN could block nuclear translocation of p65.

4 | DISCUSSION

This study showed that chronic inflammation due to continuous infusion of polyethylene particles for 6 weeks resulted in a lower BMD, as well as an increase in TRAP staining positive cells, indicating osteoclastogenesis, compared to treatment group without particles. In addition, the prevalence of the M1 pro-inflammatory macrophage phenotype was increased in particle-associated chronic inflammation. Although we have also published the continuous infusion of polyethylene particles for up to 8 weeks,[23] to keep the risk for mice to a minimum, we adopted a total 6 weeks experimental period in the current study. Delayed timing of local infusion of NF-κB Decoy ODN for the last 3 weeks was definitively shown to suppress polyethylene-particle associated chronic inflammatory osteolysis. This in vivo study using the murine femoral intramedullary continuous polyethylene particle infusion model with total 6-week-experimental period is the first to demonstrate that osteolysis due to chronic inflammation can be effectively modulated via the delayed timing of interference with the NF-κB pathway for the last 3 weeks; this minimally invasive intervention could potentially be an efficacious therapeutic strategy for periprosthetic osteolysis after TJA.

Exposure of macrophages to wear particles from orthopedic implants induced increased level of TNF-α and IL-6, leading to the stimulation of NF-κB downstream in macrophages.[14] This enhances the expression of cytokines and chemokines that lead to the further recruitment of macrophages and stimulation of osteoclastogenesis. ODNs are molecules that can prevent the binding of NF-κB to the promoter regions of targeted genes, leading to the suppression of genetic activation.[10,11] Previous studies have implicated the NF-κB pathway in acute inflammation, using the murine calvarial model and the murine femoral intramedullary continuous polyethylene particle infusion model, including increased numbers of osteoclasts and activation of RANK-RANKL-OPG cascade.[12] Polyethylene particles induced increased osteoclastogenesis via activation of the NF-κB pathway in our previous in vitro study, while NF-κB decoy ODN was found to mitigate osteoclastogenesis.[10] In the current in vivo study simulating chronic particle associated inflammation, local delivery of NF-κB decoy ODN reduced osteoclastogenesis and decreased osteolysis.

In concordance with our previous in vitro study,[10] the ALP positive area increased in the decoy ODN group with cPE compared to the treatment group with cPE; this result is consistent with the BMD findings in the current study. Interestingly, the percentage of ALP positive area did not increase significantly after the delivery of NF-κB decoy ODN in the in vivo models that simulated acute inflammation.[12–14] Acute inflammation and subsequent resolution are essential for tissue repair.[28–30] In this in vivo experiment, the delayed timing of local infusion of NFκB decoy ODN for the last 3 weeks under conditions of chronic inflammation could help resolve the inflammation and initiate the repair process. This

suggests that the timing of local delivery of NF-κB decoy ODN is critical to enhance bone healing and limit osteolysis after TJA.

Lower BMD values have been reported during acute inflammation in both the murine calvarial model[12] and the murine femoral intramedullary continuous polyethylene particle infusion model.[13,14]

The current study showed that BMD values significantly decreased due to polyethylene particles during chronic inflammation; BMD in the decoy ODN group with cPE demonstrated a reversal of the adverse effects of polyethylene particles. Interestingly, BMD in the decoy ODN group without cPE also increased. Considering both BSA and PBS were infused into the intramedullary space as carriers in all groups, the finding that local infusion of NF-κB decoy ODN could suppress ongoing low-grade chronic inflammation due to the surgical insult alone.

Recent studies consider successful bone healing to be based on the crosstalk between macrophages and cells related to bone regeneration and remodeling including osteoclasts and osteoblasts.[9,31,32] In the context of inflammation, the functional plasticity of macrophages has been emphasized.[9,31–33] A previous murine model which simulated tibial fracture with severe damage in muscle showed that persistence of the M1 pro-inflammatory macrophage phenotype resulted in poor bone healing.[34] In the current study, both the total number of macrophages and the proportion of M1 pro-inflammatory macrophages increased, while the proportion of M2 anti-inflammatory macrophages decreased in the treatment group with cPE. These findings are consistent with the increase of TRAP staining positive cells and lower BMD values associated with chronic inflammation induced by the infusion of polyethylene particles for 6 weeks. Conversely, the local delivery of NF-κB decoy ODN was found to reverse both the infiltration of macrophages and polarization to the M1 pro-inflammatory macrophage phenotype during chronic inflammation. Therefore, modulation of the M1 pro-inflammatory macrophage phenotype into the M2 anti-inflammatory macrophage phenotype during chronic inflammation could mitigate osteoclastogenesis and osteolysis and facilitate bone healing.

Polyethylene particles are the most common biomaterial associated with periprosthetic osteolysis in the clinical setting.[35] In the current study, the average size of polyethylene particles (4.62 ± 3.76 μm) is larger than that in the clinical situation in the patients with osteolysis (less than 0.95 μm). However, in our previous in vitro study, the same larger-sized polyethylene particles contaminated by endotoxin demonstrated significant pro-inflammatory marker expression, and were capable of being phgocytosed.[16,17] Xing et al also demonstrated that systemic or local administration of LPS adversely affected bone remodeling in the region, including polyethylene particles and titanium alloy rods that, were inserted into femur of rats.[36] In fact, the current in vivo study also demonstrated increased osteoclastogenesis as well as polarization of macrophages to an Ml-pro-inflammatory phenotype using these larger-sized particles. Considering that the availability of hip joint simulator-based polyethylene particles is greatly constrained due to limited production of wear debris with cross-linking of the polymer,[37] use of manufactured polyethylene particles together with LPS is a satisfactory substitute to induce inflammation and simulate osteolysis.

In addition, Kobayashi et al showed that nine of the 74 cases who were diagnosed as“aseptic loosening” prior to revision surgery actually had bacterial DNA present by polymerase chain reaction assays.[38] Gram-negative bacteria containing LPS on the outer membrane can also be present in the systemic circulation due to wounding of the skin, dental infections, after a large fatty meal or after infections of the urinary tract etc[39,40]. Therefore, polyethylene particles with low levels of LPS can also simulate aseptic loosening without evidence of laboratory nor clinically diagnosed joint infection.

The present study has several limitations. First, this murine model attempts to simulate chronic inflammatory bone loss caused by wear particle after TJA. This in vivo model is short-term, and does not reproduce exactly all of the longer-term biological processes associated with periprosthetic osteolysis in humans. In reality, the implant, or the bone bed, is loaded and the mechanical forces could also have a protective effect, especially in case of a stable prosthesis. Second, the degree of chronic inflammation was confirmed by the histological assessment of the local tissues; whether there were biomarkers of inflammation systemically was not explained. However, systemic markers of particle associated periprosthetic osteolysis are not important to the diagnosis and treatment of periprosthetic osteolysis in humans. In addition, a single time point analysis at 6 weeks was conducted in the current study. Ideally, several time points of analysis be even more informative; however, the financial and animal number aspects and restrictions of the study were prohibitive. The current study demonstrated that in the treatment group with cPE, the BMD significantly decreased and the number of TRAP staining positive cells increased compared to the treatment group without cPE groups at 6 weeks. Thus, the current experimental model could simulate inflammatory osteolysis due to wear particles reliably, similar to the clinical situation. Third, we evaluated the M1 pro-inflammatory macrophage phenotype and the M2 anti-inflammatory macrophage phenotype separately, considering potential interference between the different immunohistochemical colors making it difficult to accurately quantify the different macrophage phenotypes on one slide. One alternative to be employed in future studies is to identify the polarization of M1 and M2 macrophages using flow cytometry.

In conclusion, chronic inflammation due to polyethylene particles resulted in lower BMD values as well as an increase in osteoclastogenesis and nuclear translocation of p65, a prolonged M1 pro-inflammatory macrophage phenotype, and a decrease of M2 anti-inflammatory macrophage phenotype using the murine femoral intramedullary continuous polyethylene particle infusion model. Delayed local infusion of NF-κB decoy ODN suppressed the chronic inflammatory response due to polyethylene particles. This strategy can provide a minimally invasive treatment for periprosthetic osteolysis, when the prosthesis is still salvageable.

ACKNOWLEDGMENT

This work was supported by NIH grants R01AR063717 and R01AR073145 and Ellenburg Chair in Surgery at Stanford.

Funding information

Ellenburg Chair in Surgery at Stanford; National Institutes of Health grants, Grant/Award Numbers: R01AR073145, R01AR063717

REFERENCES

1. Goodman SB. Wear particles, periprosthetic osteolysis and the immune system. Biomaterials. 2007;28(34):5044–5048. [PubMed: 17645943]
2. Kurtz SM, Ong KL, Lau E, Bozic KJ. Impact of the economic downturn on total joint replacement demand in the United States: updated projections to 2021. J Bone Joint Surg Am. 2014;96(8):624–630. [PubMed: 24740658]
3. Abu-Amer YNF-kappaB signaling and bone resorption. Osteoporos Int. 2013;24(9):2377–2386. [PubMed: 23468073]
4. Kumar A, Takada Y, Boriek AM, Aggarwal BB. Nuclear factor-kappaB: its role in health and disease. J Mol Med. 2004;82(7):434–448. [PubMed: 15175863]
5. Xu J, Wu HF, Ang ES, et al.NF-kappaB modulators in osteolytic bone diseases. Cytokine Growth Factor Rev. 2009;20(1):7–17. [PubMed: 19046922]
6. Goodman SB, Gibon E, Yao Z. The basic science of periprosthetic osteolysis. Instr Course Lect. 2013;62:201–206. [PubMed: 23395025]
7. Clohisy JC, Hirayama T, Frazier E, Han SK, Abu-Amer Y. NF-kB signaling blockade abolishes implant particle-induced osteoclastogenesis. J Orthop Res. 2004;22(1):13–20. [PubMed: 14656654]
8. Nakashima Y, Sun DH, Trindade MC, et al.Signaling pathways for tumor necrosis factor-alpha and interleukin-6 expression in human macrophages exposed to titanium-alloy particulate debris in vitro. J Bone Joint Surg Am. 1999;81(5):603–615. [PubMed: 10360689]
9. Pajarinen J, Lin T, Gibon E, et al.Mesenchymal stem cell-macrophage crosstalk and bone healing. Biomaterials. 2019;196:80–89. [PubMed: 29329642]
10. Lin T-H, Sato T, Barcay KR, et al.NF-κB decoy Oligodeoxynucleotide enhanced osteogenesis in mesenchymal stem cells exposed to polyethylene particle. Tissue Eng Part A. 2015;21(5–6):875–883. [PubMed: 25518013]
11. Lin T-h, Yao Z, Sato T, et al.Suppression of wear-particle-induced pro-inflammatory cytokine and chemokine production in macrophages via NF-κB decoy oligodeoxynucleotide: a preliminary report. Acta Biomater. 2014;10(8):3747–3755. [PubMed: 24814879]
12. Sato T, Pajarinen J, Lin T-h, et al.NF-κB decoy oligodeoxynucleotide inhibits wear particle-induced inflammation in a murine calvarial model. J Biomed Mater Res A. 2015;103(12):3872–3878. [PubMed: 26123702]
13. Lin T, Pajarinen J, Nabeshima A, et al.Orthopaedic wear particle-induced bone loss and exogenous macrophage infiltration is mitigated by local infusion of NF-kappaB decoy oligodeoxynucleotide. J Biomed Mater Res A. 2017;105(11):3169–3175. [PubMed: 28782280]
14. Lin TH, Pajarinen J, Sato T, et al.NF-kappaB decoy oligodeoxynucleotide mitigates wear particle-associated bone loss in the murine continuous infusion model. Acta Biomater. 2016;41: 273–281. [PubMed: 27260104]
15. Shimizu H, Nakagami H, Morita S, et al.New treatment of periodontal diseases by using NF-kappaB decoy oligodeoxynucleotides via prevention of bone resorption and promotion of wound healing. Antioxid Redox Signal. 2009;11(9):2065–2075. [PubMed: 19186992]
16. Lin T, Kohno Y, Huang JF, et al.Preconditioned or IL4-secreting mesenchymal stem cells enhanced osteogenesis at different stages. Tissue Eng Part A. 2019;25(15–16):1096–1103. [PubMed: 30652628]
17. Lin T, Kohno Y, Huang JF, et al.NFkappaB sensing IL-4 secreting mesenchymal stem cells mitigate the pro-inflammatory response of macrophages exposed to polyethylene wear particles. J Biomed Mater Res A. 2018;106(10):2744–2752. [PubMed: 30084534]
18. Greenfield EM, Beidelschies MA, Tatro JM, Goldberg VM, Hise AG. Bacterial pathogen-associated molecular patterns stimulate biological activity of orthopaedic wear particles by activating cognate toll-like receptors. J Biol Chem. 2010;285(42):32378–32384. [PubMed: 20729214]

19. Gibon E, Ma T, Ren PG, et al.Selective inhibition of the MCP-1-CCR2 ligand-receptor axis decreases systemic trafficking of macrophages in the presence of UHMWPE particles. J Orthop Res. 2012;30(4):547–553. [PubMed: 21913218]
20. Gibon E, Yao Z, Rao AJ, et al.Effect of a CCR1 receptor antagonist on systemic trafficking of MSCs and polyethylene particle-associated bone loss. Biomaterials. 2012;33(14):3632–3638. [PubMed: 22364730]
21. Ma T, Huang Z, Ren PG, et al.An in vivo murine model of continuous intramedullary infusion of polyethylene particles. Biomaterials. 2008; 29(27):3738–3742. [PubMed: 18561997]
22. Nabeshima A, Pajarinen J, Lin TH, et al.Mutant CCL2 protein coating mitigates wear particle-induced bone loss in a murine continuous polyethylene infusion model. Biomaterials. 2017;117:1–9. [PubMed: 27918885]
23. Pajarinen J, Nabeshima A, Lin TH, et al.(*) murine model of progressive orthopedic wear particle-induced chronic inflammation and Osteolysis. Tissue Eng Part C Methods. 2017;23(12):1003–1011. [PubMed: 28978284]
24. Ren PG, Irani A, Huang Z, Ma T, Biswal S, Goodman SB. Continuous infusion of UHMWPE particles induces increased bone macrophages and osteolysis. Clin Orthop Relat Res. 2011;469(1):113–122. [PubMed: 21042895]
25. Sato T, Pajarinen J, Behn A, et al.The effect of local IL-4 delivery or CCL2 blockade on implant fixation and bone structural properties in a mouse model of wear particle induced osteolysis. J Biomed Mater Res A. 2016;104(9):2255–2262. [PubMed: 27114284]
26. Ueno M, Lo CW, Barati D, et al.Interleukin-4 overexpressing mesenchymal stem cells within gelatin-based microribbon hydrogels enhance bone healing in a murine long bone critical-size defect model. J Biomed Mater Res A. 2020;108(11):2240–2250. [PubMed: 32363683]
27. Giridharan S, Srinivasan M. Mechanisms of NF-kappaB p65 and strategies for therapeutic manipulation. J Inflamm Res. 2018;11:407–419. [PubMed: 30464573]
28. Bahney CS, Zondervan RL, Allison P, et al.Cellular biology of fracture healing. J Orthop Res. 2019;37(1):35–50. [PubMed: 30370699]
29. Fullerton JN, Gilroy DW. Resolution of inflammation: a new therapeutic frontier. Nat Rev Drug Discov. 2016;15(8):551–567. [PubMed: 27020098]
30. Maruyama M, Rhee C, Utsunomiya T, et al.Modulation of the inflammatory response and bone healing. Front Endocrinol. 2020;11:386.
31. Loi F, Cordova LA, Pajarinen J, Lin TH, Yao Z, Goodman SB. Inflammation, fracture and bone repair. Bone. 2016;86:119–130. [PubMed: 26946132]
32. Mosser DM, Edwards JP. Exploring the full spectrum of macrophage activation. Nat Rev Immunol. 2008;8(12):958–969. [PubMed: 19029990]
33. Dorrington MG, Fraser IDC. NF-kappaB signaling in macrophages: dynamics, crosstalk, and signal integration. Front Immunol. 2019; 10:705. [PubMed: 31024544]
34. Hurtgen BJ, Ward CL, Garg K, et al.Severe muscle trauma triggers heightened and prolonged local musculoskeletal inflammation and impairs adjacent tibia fracture healing. J Musculoskelet Neuronal Interact. 2016;16(2):122–134. [PubMed: 27282456]
35. Willert HG, Bertram H, Buchhorn GH. Osteolysis in alloarthroplasty of the hip. The role of ultra-high molecular weight polyethylene wear particles. Clin Orthop Relat Res. 1990;258:95–107.
36. Xing Z, Pabst MJ, Hasty KA, Smith RA. Accumulation of LPS by polyethylene particles decreases bone attachment to implants. J Orthop Res. 2006;24(5):959–966. [PubMed: 16609962]
37. von Knoch M, Jewison DE, Sibonga JD, et al.The effectiveness of polyethylene versus titanium particles in inducing osteolysis in vivo. J Orthop Res. 2004;22(2):237–243. [PubMed: 15013080]
38. Kobayashi N, Procop GW, Krebs V, Kobayashi H, Bauer TW. Molecular identification of bacteria from aseptically loose implants. Clin Orthop Relat Res. 2008;466(7):1716–1725. [PubMed: 18438724]
39. Farnsworth CW, Schott EM, Benvie AM, et al.Obesity/type 2 diabetes increases inflammation, periosteal reactive bone formation, and osteolysis during Staphylococcus aureus implant-associated bone infection. J Orthop Res. 2018;36(6):1614–1623. [PubMed: 29227579]
40. Marmor S, Kerroumi Y. Patient-specific risk factors for infection in arthroplasty procedure. Orthop Traumatol Surg Res. 2016;102(1 Suppl):S113–S119. [PubMed: 26867708]

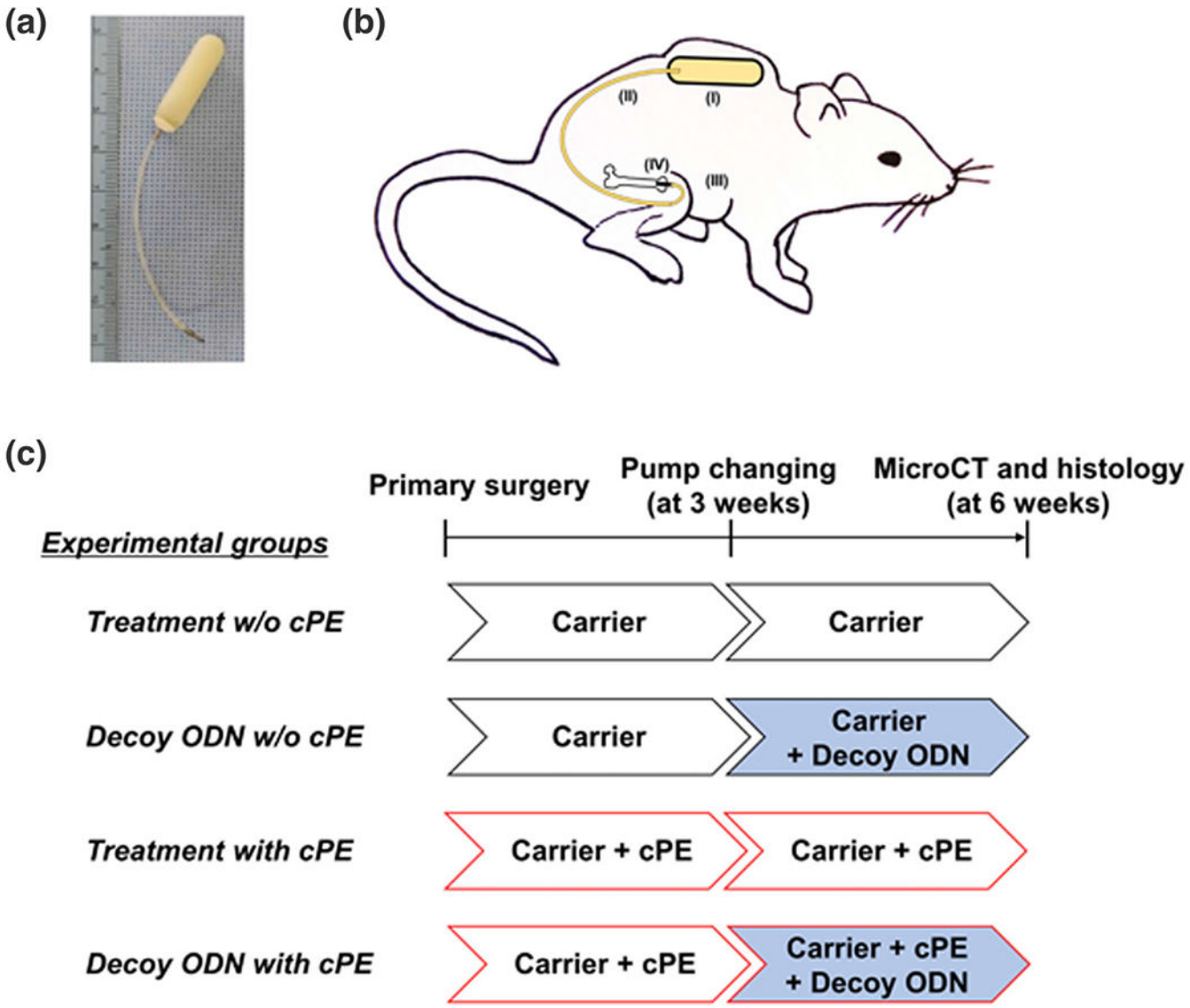

FIGURE 1.

Murine continuous polyethylene particle infusion model that causes chronic inflammation. (a) Implants used in this model include a diffusion pump containing contaminated polyethylene particles (cPE, 1.25% of polyethylene particles and 10 ng/ml of lipopolysaccharides) or carrier, 6 cm of vinyl catheter and the hollow titanium rod (length: 6 mm, diameter: 23 gauge). (b) Schematic drawing of the murine femoral continuous intramedullary particle infusion model. An osmotic pump containing contaminated polyethylene particles or carrier alone was subcutaneously implanted in the dorsal side of the mouse (I). Using a subcutaneous vinyl catheter tubing (II), the osmotic pump is then connected with the hollow titanium rod (III) which is pressed fit into the medullary cavity of the right distal femur (IV). (c) Groups and timeline. There were four groups with/without cPE and with/without treatment of nuclear factor kappa B (NF-κB) decoy oligodeoxynucleotide (ODN) (50 μM) as follows: (1) treatment group without cPE, (2) infusion of decoy ODN at 3 weeks after primary surgery without cPE, (3) treatment

group with cPE, and (4) infusion of decoy ODN at 3 weeks after primary surgery with cPE. Each group included seven mice. Carrier for the particles was 10% BSA/PBS; ODN, Oligodeoxynucleotide; cPE, Contaminated polyethylene particle with LPS. For the delivery of the NF-κB decoy ODN at 3 weeks after primary surgery, pumps were replaced to new ones containing NF-κB decoy ODN, which was infused for three more weeks in groups (2) and (4). Pumps were also replaced with new ones containing the same infusion as first 3 weeks in groups (1) and (3) for three more weeks. micro-computational tomography (MicroCT) and immunohistochemical analysis were performed 6 weeks after primary surgery

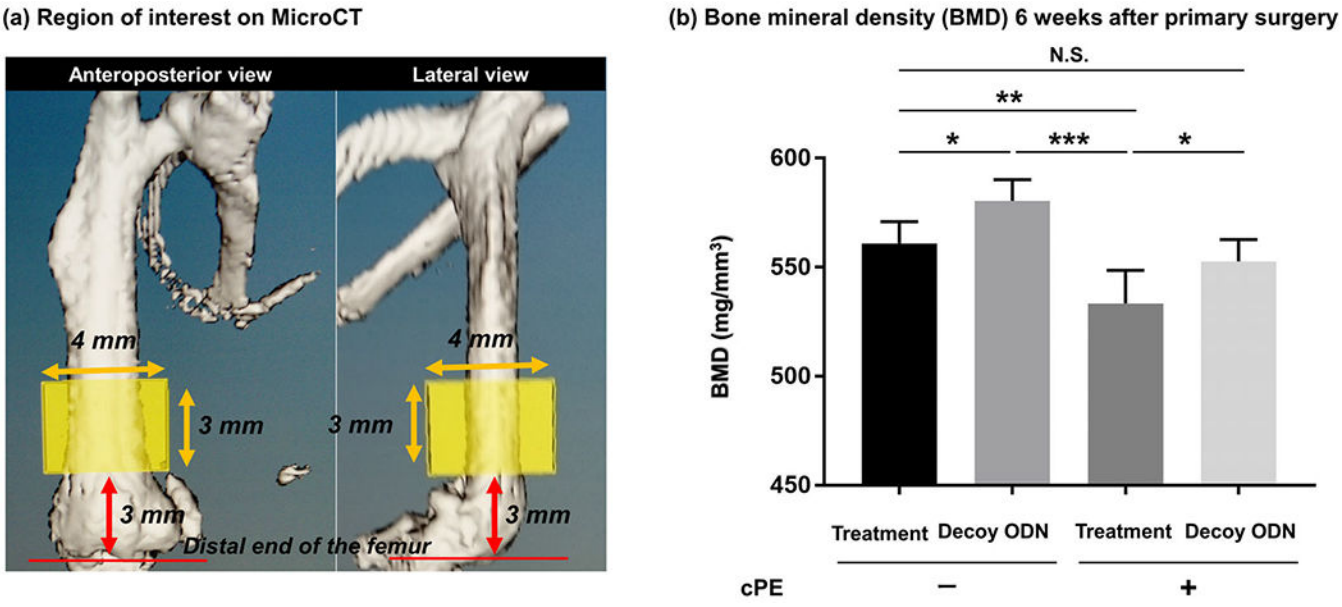

FIGURE 2.

Micro-computational tomography (MicroCT) analysis. (a) MicroCT scanning was performed 6 weeks after the primary surgery. A three-dimension (3D) region of interest (ROI) was created using a rectangular parallelepiped (height: 3 mm, width: 4 mm, depth: 3 mm) within the diaphysis. The distal end of 3D-ROI was set 3 mm proximally from the distal end of the femoral condyles along the longitudinal axis of the femur. The bone mineral density (BMD, mg/mm^3) was assessed using the GEMS MicroView software in which threshold was set as 700 HU. (b) Local delivery of nuclear factor kappa B (NF-κB) decoy ODN mitigated chronic inflammatory bone loss induced by cPE. Quantitative assessment of bone mineral density (BMD) in all groups. *$p < 0.05$, **$p < 0.001$, ***$p < 0.0001$

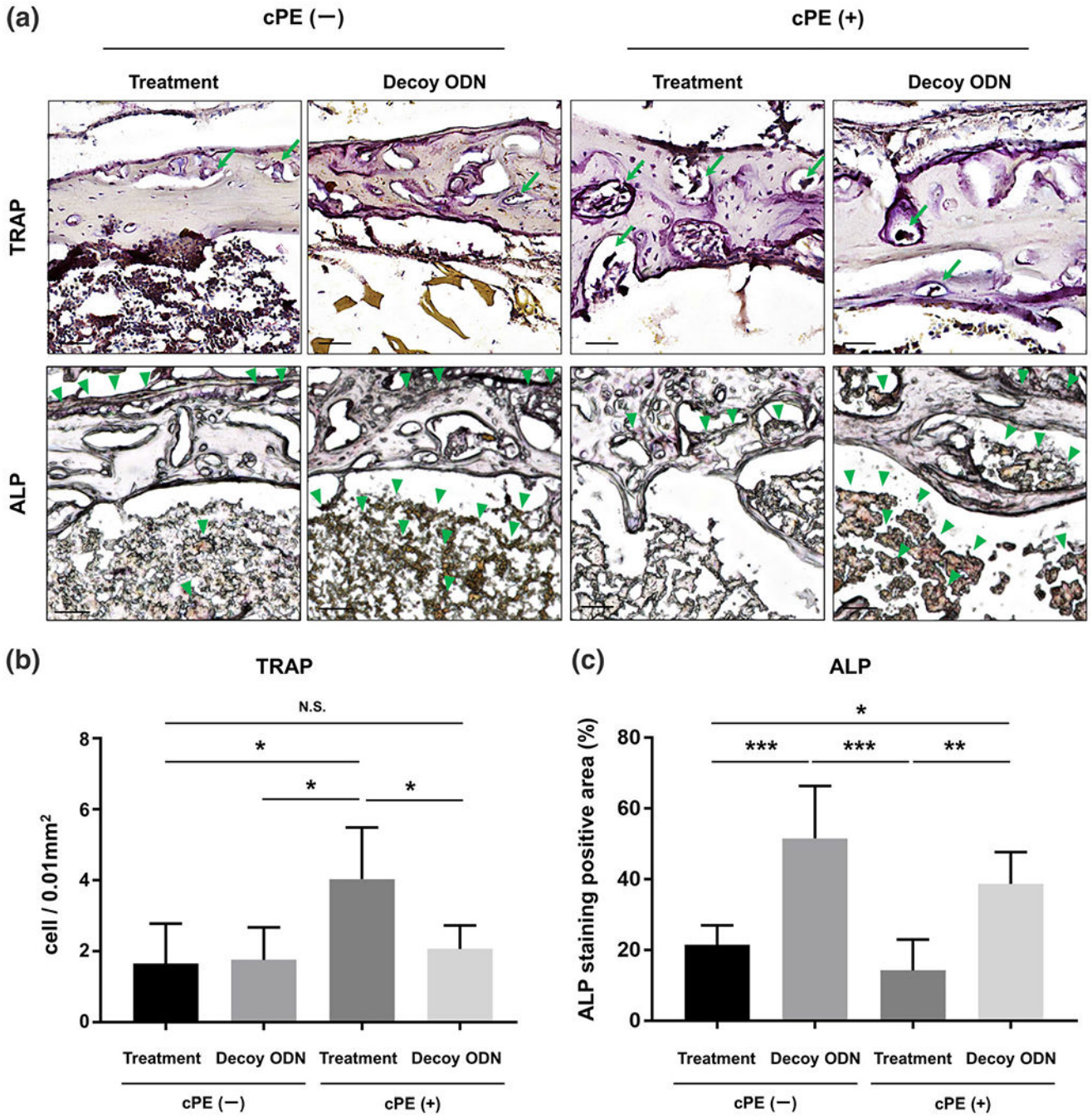

FIGURE 3.

Local delivery of nuclear factor kappa B (NF-κB) decoy oligodeoxynucleotide (ODN) mitigated the number of osteoclast-like cells induced by cPE and increased the percentage of anti-alkaline phosphatase (ALP) staining positive area in chronic inflammation. Representative pictures of TRAP and ALP staining in all groups (a). Leukocyte tartrate resistant acid phosphatase (TRAP) staining was used to identify the osteoclast-like cells with multi-nuclei stained brown (arrows), which were located on the bone perimeter within the resorption lacunae in the upper photomicrographs. Osteoblast-like cells were stained brown

(arrowheads) by ALP staining in the lower photomicrographs. (b) Quantitative assessment for cells positively stained with TRAP. Using three randomly selected views with ×200 magnification in each specimen, in a blind manner, two investigators manually counted the number of TRAP staining positive cells, which were finally normalized by the bone area measured using the ImageJ software (National Institutes of Health). (c) Quantitative assessment of the percentage of ALP staining positive area based on based on the whole area of each specimen. Using the entire image of each specimen with ×100 magnification, the percentage of brown, positively stained area (arrowheads) for ALP was also quantified based on the entire area of each section measured using the ImageJ software (National Institutes of Health). Color threshold of ALP staining positive area was determined by consensus of three of the investigators. Black bar: 50 μm. *$p < 0.05$, **$p < 0.001$, ***$p < 0.0001$

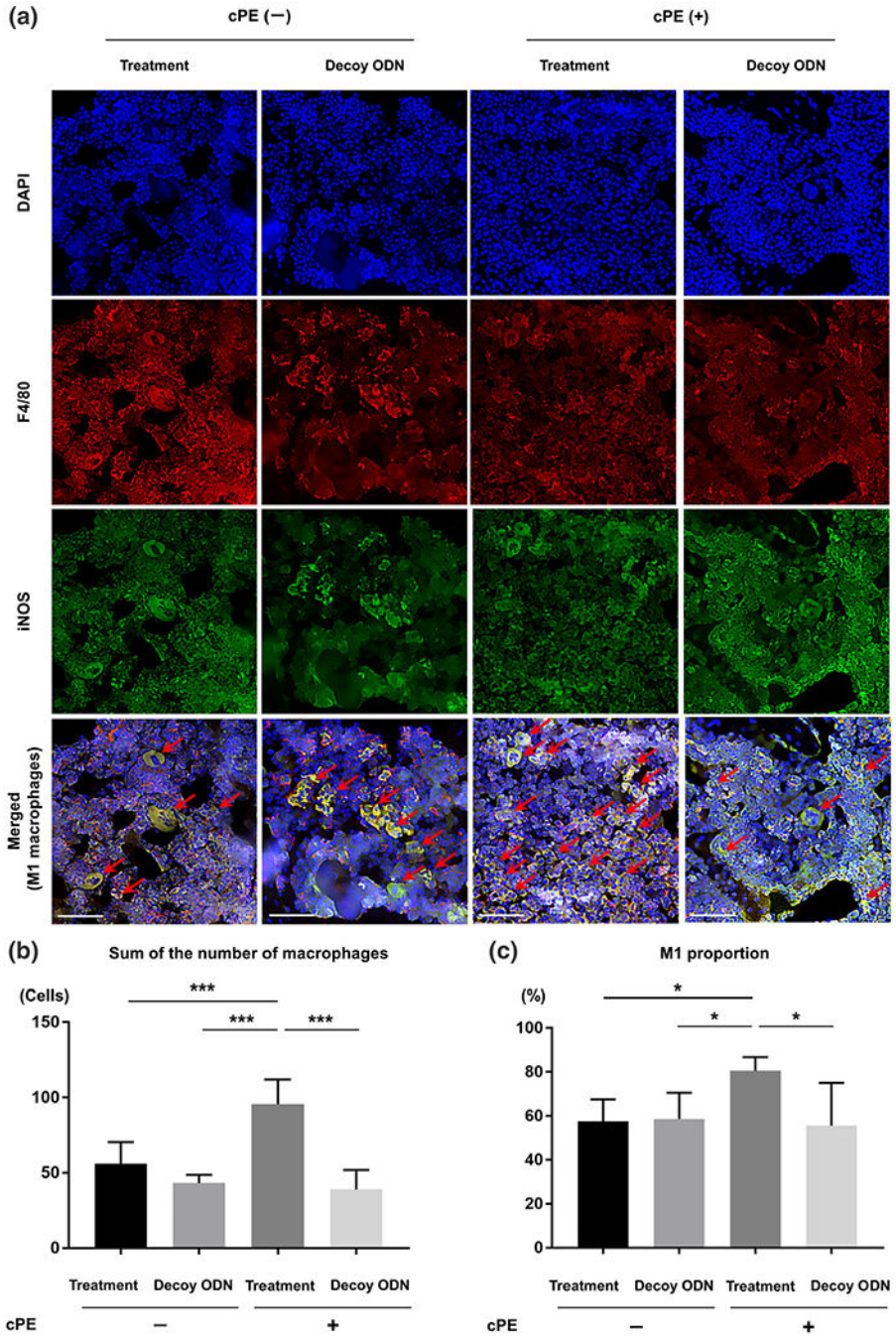

FIGURE 4.

Photomicrographs and graphs showing M1 pro-inflammatory macrophages. Immunofluorescence staining of anti-F4/80 antibody (red) and anti-inducible nitric oxide synthase (iNOS) antibody (green) was used to identify the M1 pro-inflammatory macrophages. DAPI (blue) was used to visualize nuclei. In merged images, the cells double positively stained with both anti-F4/80 antibody and anti-iNOS antibody indicated M1 pro-inflammatory macrophages (arrow) (a). In this section, quantitative assessments of macrophages (the sum of the number of cells positively stained with F4/80 and the number

of cells double positively stained with both F4/80 and iNOS) (b) and the proportion of M1 pro-inflammatory macrophages (based on the following calculation: the number of cells double positively stained with both F4/80 (red) and iNOS divided by the sum of the number of cells positively stained with F4/80 and the number of cells double positively stained with both F4/80 and iNOS) (c) were also shown based on manually counting in three randomly selected views of each specimen with ×200 magnification by ImageJ software. White bar: 50 μm. *$p < 0.05$, **$p < 0.001$, ***$p < 0.0001$

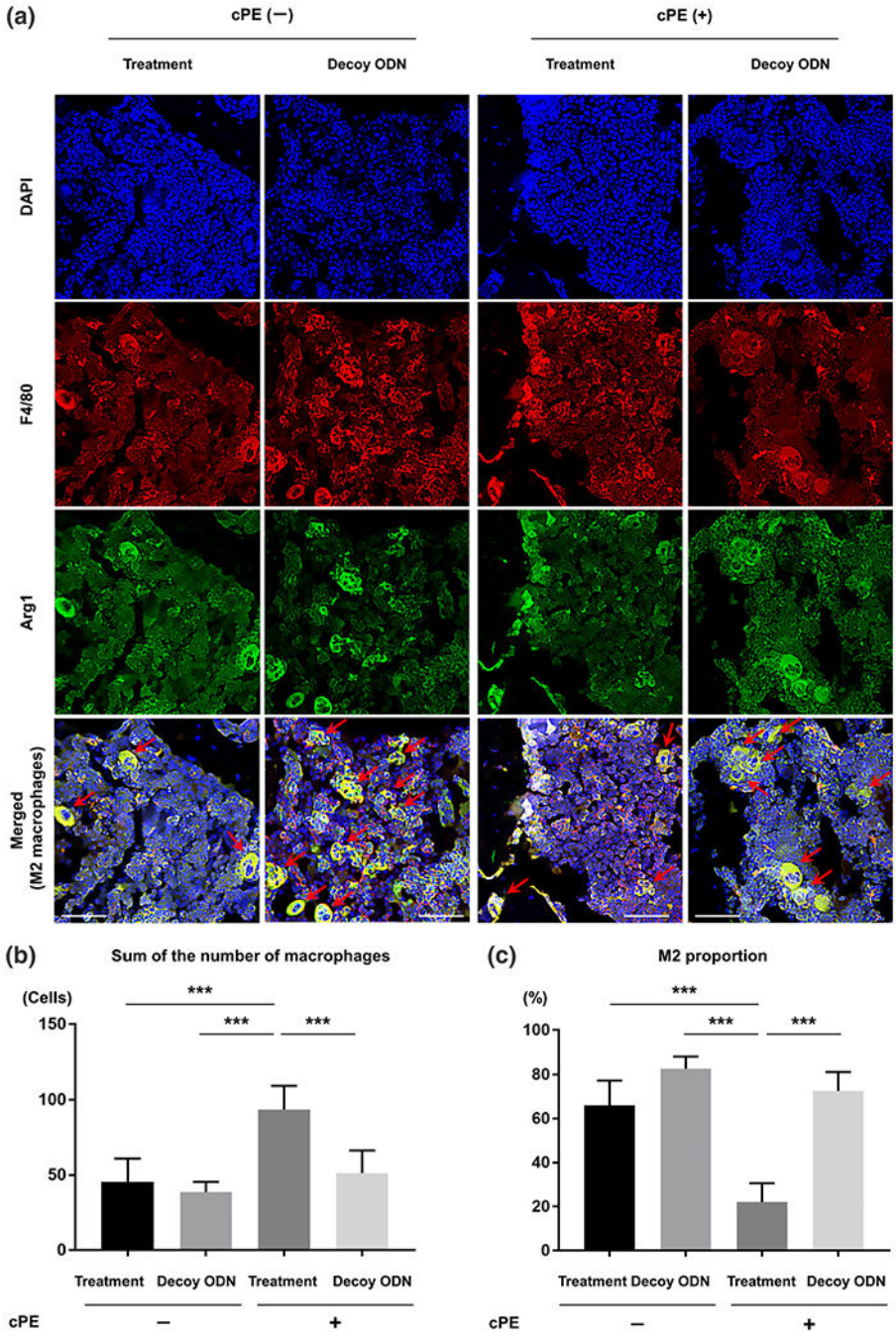

FIGURE 5.

Photomicrographs and graphs showing the M2 anti-inflammatory macrophages. In different sections, immunofluorescence staining of anti-F4/80 antibody (red) and anti-liver arginase (Arg1) polyclonal antibody (green) was used to identify the M2 anti-inflammatory macrophages. DAPI (blue) was used to visualize nuclei. In merged images, the cells double positively stained with both anti-F4/80 antibody and anti-Arg1 antibody indicated the M2 anti-inflammatory macrophages (arrow) (a). Using this section, quantitative assessments of macrophages (the sum of the number of cells positively stained with F4/80 and the number

of cells double positively stained with both F4/80 and Arg1) (b) and the proportion of M2 anti-inflammatory macrophages (based on the following calculation: The number of cells double positively stained with both F4/80 and Arg1 divided by the sum of the number of cells positively stained with F4/80 and the number of cells double positively stained with both F4/80 and Arg1) (c) were also shown based on manually counting in three randomly selected views of each specimen with ×200 magnification by ImageJ software. White bar: 50 μm. *$p < 0.05$, **$p < 0.001$, ***$p < 0.0001$

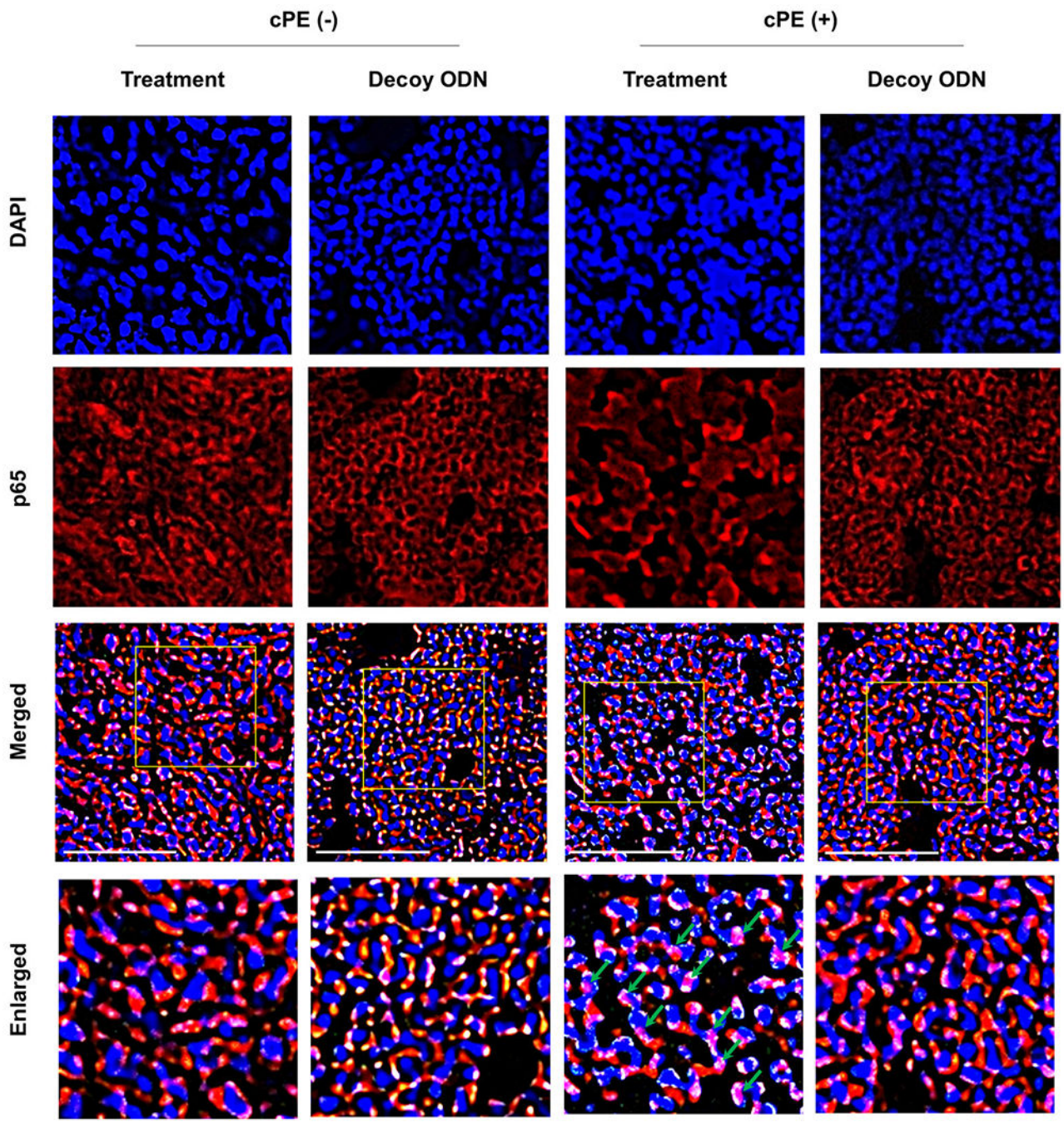

FIGURE 6.

Photomicrographs showing the distribution of p65. Sections were stained with anti-p65 staining (red) and nuclei are visualized with DAPI (blue). In merged images, the overlapping of anti-p65 staining (red) and nuclei stained with DAPI (blue) showed pink color (green arrow), indicating that p65 was located within nuclei (nuclear translocation of p65). In the treatment group with cPE, nuclear translocation of p65 was markedly observed (pink). On the other hand, in the other groups, anti-p65 staining (red) was located mainly outside of nuclei stained with DAPI (blue). Notably, in nuclear factor kappa B (NF-κB) decoy

oligodeoxynucleotide (ODN) treatment groups with cPE, the overlapping color (pink) of anti-p65 staining (red) and nuclei stained with DAPI (blue) was less compared to that in the treatment group with cPE. It indicated that local infusion of NF-κB decoy ODN could block nuclear translocation of p65 after cPE stimulation. White bar: 50 μm

TABLE 1

Survey of the literatures using a murine continuous polyethylene particle infusion model: Comparison with the current study in terms of therapeutic intervention and its timing

Authors [ref.]	Publication year	Experimental period	Therapeutic intervention	Delivering method of therapeutic intervention	Timing of therapeutic intervention
Ma T[21]	2008	4 weeks	NA	NA	NA
Ren PG [24]	2011	25 days	NA	NA	NA
Pajarinen J [23]	2017	8 weeks	NA	NA	NA
Gibon E [19]	2012	5 weeks	Antagonist of the MCP-1 receptor	Daily intraperitoneal injection or daily intravenous injection	Beginning 2 weeks before surgery and 3 weeks after surgery
Gibon E [20]	2012	5 weeks	Antagonist of the CCR1 receptor	Daily intraperitoneal injection	Beginning 1 week before surgery and 4 weeks after surgery
Sato T [25]	2016	4 weeks	IL-4 7ND-releasiug coating titanium rod	Continuous intramedurally infusion Press-fit into the femur	Day 0–4 weeks after primary surgery Day 0–4 weeks after primary surgery
Nabeshima A [22]	2017	4 weeks	7ND-releasiug coating titanium rod	Press-fit into the femur	Day 0–4 weeks after primary surgery
Lin T [13]	2017	3 weeks	NF-κB decoy ODN	Continuous intramedurally infusion	Day 0–3 weeks after primary surgery
Lin T [14]	2016	4 weeks	NF-κB decoy ODN	Continuous intramedurally infusion	Day 0–4 weeks after primary surgery
The current study		6 weeks	NF-κB decoy ODN	Continuous intramedurally infusion	4–6 weeks after primary surgery

Abbreviations: CCR1, C—C motif receptor 1; IL-4, interleukin-4; MCP-1, monocyte chemoattractant protein-1; NA, not available; NF-κB, nuclear factor kappa B; ODN, oligodeoxynucleotide.